Cerebral Cortex April 2006;16:447–459
doi:10.1093/cercor/bhi124
Advance Access publication June 15, 2005

Distribution of Activity Across the Monkey Cerebral Cortical Surface, Thalamus and Midbrain during Rapid, Visually Guided Saccades

Justin T. Baker[1], Gaurav H. Patel[2], Maurizio Corbetta[1,2] and Lawrence H. Snyder[1]

[1]Department of Anatomy & Neurobiology, Washington University School of Medicine, St Louis, MO, USA and [2]Department of Neurology & Neurological Surgery, Washington University School of Medicine, St Louis, MO, USA

To examine the distribution of visual and oculomotor activity across the macaque brain, we performed functional magnetic resonance imaging (fMRI) on awake, behaving monkeys trained to perform visually guided saccades. Two subjects alternated between periods of making saccades and central fixations while blood oxygen level dependent (BOLD) images were collected [3 T, (1.5 mm)^3 spatial resolution]. BOLD activations from each of four cerebral hemispheres were projected onto the subjects' cortical surfaces and aligned to a surface-based atlas for comparison across hemispheres and subjects. This surface-based analysis revealed patterns of visuo-oculomotor activity across much of the cerebral cortex, including activations in the posterior parietal cortex, superior temporal cortex and frontal lobe. For each cortical domain, we show the anatomical position and extent of visuo-oculomotor activity, including evidence that the dorsolateral frontal activation, which includes the frontal eye field (on the anterior bank of the arcuate sulcus), extends anteriorly into posterior principal sulcus (area 46) and posteriorly into part of dorsal premotor cortex (area 6). Our results also suggest that subcortical BOLD activity in the pulvinar thalamus may be lateralized during voluntary eye movements. These findings provide new neuroanatomical information as to the complex neural substrates that underlie even simple goal-directed behaviors.

Keywords: fMRI, macaque, oculomotor, vision, saccades

Introduction

Each visually guided eye movement is produced by a cascade of events starting at the retina, passing through a network of brain areas to ultimately cause a coordinated, ballistic contraction of the extraocular muscles. Although a visually guided saccade appears to be the epitome of a simple sensory-to-motor transformation, it nonetheless involves the activation of brain regions distributed across all levels of the nervous system (except the spinal cord), including the frontal and parietal cortices of both cerebral hemispheres, their diencephalic targets in the medial dorsal and lateral pulvinar thalamus, as well as the basal ganglia, midbrain and cerebellum (for a review, see Munoz, 2002). This broadly distributed neural architecture attests to the complex nature of goal-oriented processing in general, even in the simple case of choosing where to move the eyes. Single-unit electrophysiology in macaque monkeys has revealed many of the details underlying goal-oriented processing in the oculomotor network. However, few studies have specifically set out to explore the distributed nature of the oculomotor system in the monkey. By providing an objective measure of relative neural activity across the entire cortical and subcortical manifolds, such studies may help to parcellate the brain areas that make up the oculomotor network in ways that would be difficult or even impossible to achieve using the single-unit approach.

Functional magnetic resonance imaging (fMRI) technology has only recently become available as a tool for studying distributed brain systems in monkeys (Vanduffel *et al.*, 2001; Nakahara *et al.*, 2002; Vanduffel *et al.*, 2002; Tsao *et al.*, 2003; Denys *et al.*, 2004; Koyama *et al.*, 2004; Pinsk *et al.*, 2005). fMRI has become the preferred method of many scientists studying the human oculomotor system, since it is completely noninvasive and can perform at higher spatial resolutions than other imaging modalities such as positron emission tomography (PET), electroencephalography or magnetoencephalography. Yet to date, most functional imaging studies using alert participants have employed humans, a species for which there is almost no neurophysiological data available at the single cell level. In contrast, there are only a small number of studies of macaque volitional behavior using brain imaging, despite the vast amount of single cell data available for monkeys. Indeed, only one study has used fMRI to map saccade-related activity across parts of the cerebral cortex (Koyama *et al.*, 2004). By providing blood oxygen level-dependent (BOLD) maps from monkeys that can be compared against the existing single unit literature, these studies will help to establish how the different signals emphasive different aspects of cellular activity, which will in turn help to establish a 'common currency' for results from human imaging and monkey neurophysiology to be compared with greater facility. As a result, a broader understanding of goal-directed behavior is likely to emerge in which the literature concerning humans and monkeys can contribute to comprehensive models of goal-directed processing.

The goal of the present study was to identify the distribution of brain activity that occurs when monkeys produce rapid eye movements in response to visual cues. Neural activity was measured using BOLD fMRI while alert monkeys performed saccades to visual targets in a simple, blocked behavioral paradigm. For cerebral cortical activity, functional data were mapped onto the cortical surface of each individual, and then combined onto a single surface to examine the consistency of saccade-related activity patterns across the two hemispheres and across our two individual subjects. Subcortical activity was also assessed for structures where sufficient signal-to-noise was available. These included the midbrain, basal ganglia and thalamus. Although this analysis revealed a constellation of active areas that was broadly consistent with our expectations based on the existing literature, our results provide this activity map in a way that exceeds both the scope and the level of detail currently available from either the single unit or imaging literatures, and thus provides an important contribution to the study of goal-directed oculomotor processing in the primate brain.

Materials and Methods

Two male cynomolgus monkeys (*Macaca fascicularis*, 3–5 kg) were used in the present study. Before training, preliminary surgery was performed under deep anesthesia with isofluorane and aseptic conditions. A post made of a high tensile strength plastic (polyetheretherketon or PEEK) for restraining the head of the monkey was implanted on the skull behind the brow ridge. It was anchored to the skull using dental acrylic and small ceramic screws (4 mm diameter, Thomas Recording GmbH, Germany). Training commenced 6–8 weeks after surgery. All experimental procedures were conducted in accordance with local and NIH guidelines.

Monkeys were trained to perform a saccade paradigm while habituating to the experimental setup in a simulated scanner (Fig. 1*A*). During daily sessions the monkey sat prone in a horizontally oriented, cylindrical monkey chair (Primatrix Inc., Melrose, MA) with its head rigidly fixed by the head post to a head holder on the chair. A plastic water spout was positioned close to the animal's mouth for the delivery of liquid reward. The chair was placed within a cylindrical tube the same diameter as the MR bore (35 cm), with the animal facing a Lucite screen mounted over one end of the tube at a distance of 55 cm from the eyes. Visual stimuli were back-projected onto the screen using a liquid crystal display projector (Sharp USA, Montclair, NJ). The experiment was controlled by two linked computers running in-house software, the first controlling the timing and storage of events and the second generating the projected visual stimuli.

Eye movements were recorded using an infrared (IR) eye tracking system (ISCAN Inc., Melrose, MA). IR light was directed at one of the eyes, either using an array of 20 IR light emitting diodes 35 cm from the animal (in the simulated scanner setup) or using a plastic fiber optic cable that delivered light from a remote source to an IR-filtered termination point 5–7 cm from the eye (in the MRI scanner). An image of the eye was captured using an IR-sensitive CCD video camera operating at 240 frames per second. The video signal was passed to a dedicated computer running the vendor's software package which computed horizontal and vertical eye position from each frame of the video image based on the angular difference between the IR reflection and the center of the pupil. These signals were digitized (500 samples/s), used to control behavioral feedback, and stored for off-line analysis along with a record of stimulus presentation times and the start time of each MR volume acquisition (see MRI Procedures). A calibration procedure was used before each session to minimize both systematic and variable errors in the eye position track.

The timing and trial types used in the behavioral paradigm are illustrated in Figure 1 (panels B,C). Saccadic eye movement trials started when the animal fixated on a central visual stimulus (a red square, 0.7 × 0.7°). After 150 ms, the stimulus stepped abruptly from the central location to one of four (M1) or eight (M2) peripheral locations spaced around a virtual circle (radius, 5–7°). After the step, the animal had 450 ms to move its eyes to the new target position (1.5 × 1.5° square window centered on the target). The target stepped back to the central position 600 ms after it appeared, and the animal again had 450 ms to return its eyes back to the central position before the start of the next trial. The animal was rewarded with a drop of juice or water for successfully completing each trial (one out and back saccade sequence). During fixation trials, rewards were provided at the same rate for keeping the eyes fixed at the central screen position. A blocked design was used to increase the magnitudes of task-related BOLD responses by summating the hemodynamic responses to closely-spaced events. Saccade and fixation trials were blocked in groups of ten, which yielded an alternating pattern of 12 s of rapid eye movements followed by 12 s of static eye position (Fig. 1*D*).

Saccades were identified from the behavioral record using a combination of displacement (a change of at least 2° after heavy low pass filtering) and velocity (20°/s after light low pass filtering) criteria. This procedure was sensitive to saccades as small as 2° in amplitude. Blinks were also identified from the record and removed from the behavioral analysis. Numbers of saccades and blinks were compared between fixation and saccade blocks to establish that the stimulus-based regressor was sufficient to measure activity related to performance of the saccade paradigm (see below).

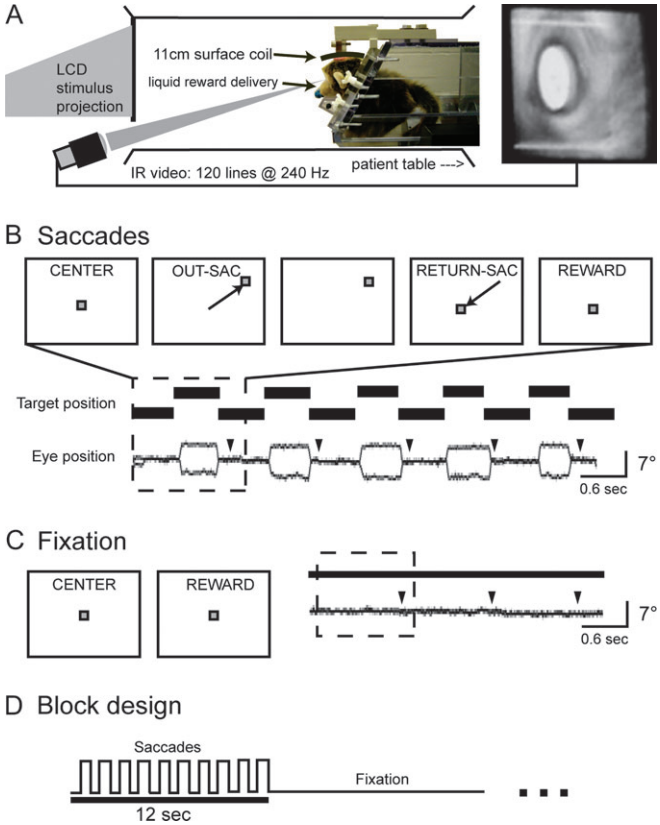

Figure 1. Behavioral paradigm and apparatus. (*A*) Experimental setup and eye movement recording. The schematic drawing shows a side view of the chair as it was positioned in the scanner and mock setups. A stuffed animal shows the typical 'sphinx-like' posture assumed by subjects: prone with the arms and chest angled up and forward and the legs and tail below and behind. The right panel shows an image of the eye captured from the IR video camera, illustrating pupil detection within a fixed portion of the video image (white overlay and box). (*B*) A saccade trial and a representative saccade sequence. The upper row of panels illustrates the sequence of events from a typical saccade trial, with two eye movements followed by a reward. The lower rows shows a sample of behavioral data from five saccade trials (dashed box shows one trial) performed inside the scanner, on which the subject (M1) was successful. Arrowheads show the timing of reward delivery. (*C*) Schematic illustration of a fixation 'trial' and a representative sample of three successful fixation trials from the same subject. (*D*) Block design. Target position (solid line) stepped back and forth from a peripheral position for a period of 12 s ('Saccades'), followed by 12 s of no movement at the center of the screen ('Fixation').

MRI Procedures

Awake behaving macaques were examined using a Siemens 3T Allegra MRI scanner (Siemens Medical Solutions, Erlangen, Germany). Head position minimized the distance between the brain center and the magnetic field center, while ensuring that the animal could sit comfortably. Functional data were collected using a gradient-echo echo-planar pulse sequence sensitive to BOLD contrast (T2*) (T2* evolution time = 25 ms, flip angle = 90°, dorsal-to-ventral phase-encoding) and a surface coil equipped to transmit and receive radio frequency signals (13 cm inner diameter; Primatrix). The coil fit around each animal's head post and was saddle-shaped to provide more extensive brain coverage as compared to planar surface coils. Fifty-six coronal slices, each with a square field of view (96 × 96 mm, 64 × 64 image matrix) and a thickness of 1.5 mm, were obtained using contiguous, interleaved acquisition, and a repetition time (T_R) of 3200 ms. This scanning protocol was chosen to cover the whole-brain at an isotropic spatial resolution [$(1.5\ \text{mm})^3$]. Ninety-four volumes were acquired in each fMRI run, the first four of which were excluded to allow for the equilibration of longitudinal magnetization. Subjects underwent between five and 15 runs per session, and were scanned over the course of several weeks in multiple functional imaging sessions. A total of 10 440 functional images were acquired.

High-resolution structural images were collected in separate sessions, during which the animal was chemically restrained (10–15 mg/kg ketamine and 0.6 mg/kg xylazine). T1-weighted images were acquired using a magnetization-prepared rapid acquisition gradient-echo pulse sequence [MP-RAGE; $(0.75\ mm)^3$ isotropic resolution, flip angle = 7°, six acquisitions] and a volumetric transmit and receive coil (16 cm i.d.; Primatrix).

Image Analysis

Each reconstructed fMRI run produced a four-dimensional (x, y, z, time) stack that was passed through four unsupervised processing steps. These steps involved (i) compensation for asynchronous slice acquisition, using sinc interpolation; (ii) debanding, which removed systematic odd versus even slice intensity differences that occur with contiguous, interleaved slice acquisition; (iii) realignment, using a six-parameter rigid body alignment algorithm to mutually register all frames in all runs for each subject; and (iv) normalization, in which the overall intensity of each four-dimensional stack was uniformly scaled to a whole brain mode value of 1000 (Ojemann *et al.*, 1997).

After these initial operations, the BOLD signal time course was spatially smoothed using a gaussian kernel (1.5 mm full width at half maximum) and then each voxel was tested for significant saccade-related activity using a general linear model (Friston *et al.*, 1995). The regressor representing the expected saccade-related hemodynamic response was derived by convolving a boxcar function representing the alternating saccade paradigm (eye movement trials = 1, fixation trials = 0) with a gamma function (time constant or scale parameter = 1.25 s, phase delay or shape parameter = 3) (Boynton *et al.*, 1996). The results of the regression analysis were converted to units of standard deviation (Ollinger *et al.*, 2001), and the resulting Z maps from each subject were co-registered on the basis of their structural scans.

Regions of interest (ROIs) were generated based on the entire data set using an established procedure (Mintun *et al.*, 1989). Individual Z-score maps were added together and then renormalized to obtain an image of saccade-related activity across the two subjects that remained in units of standard deviation (by dividing the sum by the square root of two). Activation peaks were next identified in the group image, using an algorithm that required local maxima peak values to be greater than $Z = 2.58$ ($P < 0.01$) and pairs of peaks to be no less than 4 mm apart. ROIs were then defined around each peak by including all voxels within 2.5 mm of the peak that were above a more modest statistical threshold ($Z > 1.96$, $P < 0.05$). An additional criterion was used to eliminate ROIs where activity was driven primarily by one subject: if only one subject showed active voxels ($P < 0.05$) within the defined ROI, this ROI was excluded from further analysis. Identifying ROIs in this fashion is intended to operationally define saccade-related brain regions in the context of this study. Response magnitude from each ROI was measured as the peak percentage change (mean over the voxels in that ROI) obtained from the amplitude of the modeled hemodynamic response that best fit the measured response.

Saccade-related activation foci were localized using both conventional and surface-based methods. Activation peak coordinates derived from the ROI analysis are reported relative to the anterior commissure. Individual subject statistical data, including Z maps and standard deviation maps, were also inspected on their own T2-weighted and T1-weighted structural images. Subcortical activation peaks were localized relative to the underlying anatomy using a published brain atlas (Paxinos *et al.*, 1999). Activation in the cerebral cortex was evaluated both in three dimensions and projected onto a surface representation of the individual's cerebral cortex using the SureFit/Caret software suite (Van Essen *et al.*, 2001). A surface-based registration procedure was used to morph each individual's cortical surface to a standard rhesus template (F99UA1, http://brainmap.wustl.edu:8081/sums/index.jsp) or atlas, thereby providing a common anatomical frame of reference for comparisons across studies and laboratories. Each hemisphere was aligned to the atlas using 12 sulcal landmarks: principal sulcus (PS), arcuate sulcus (AS) and spur, central sulcus (CS), cingulate sulcus (CingS), intraparietal sulcus (IPS), lunate sulcus (LS), parieto-occipital sulcus (POS), superior temporal sulcus (STS), sylvian fissure (SF), calcarine sulcus (CaS) and inferior occipital sulcus (IOS). Activations were then assigned to areas based on a previous anatomical study (Felleman and Van Essen, 1991).

Results

The purpose of the present study was to examine the distribution of saccade-related brain activity in the behaving macaque monkey. Animals made visually guided eye movements while fMRI was used to measure BOLD signals associated with task performance. In alternating blocks lasting 12 s each, the visual target either stepped back and forth every 600 ms between a central position and one of four peripheral positions or remained fixed at the central position. The BOLD signal time course was analyzed for saccade-related activity, and significant responses were mapped onto structural scans to localize the saccade-related network with respect to brain anatomy.

Behavioral Results

Subjects performed a total of 1441 saccade blocks and 1343 fixation blocks over 16 separate functional imaging sessions. Subjects generally performed well in the scanner for up to 2 h.

Both subjects made many more saccades during eye movement blocks than during fixation blocks [M1, movement (18.5 ± 5.4, mean ± SD saccades per block) versus fixation (2.9 ± 2.2), $P < 0.001$; M2, movement (17.7 ± 2.9) versus fixation (3.5 ± 2.7), $P < 0.001$] (Fig. 2*A*). Figure 2*B* shows the distribution of saccade endpoints obtained from one animal; the central circle devoid of endpoints is the fixation window. During saccade and fixation blocks, each animal made similar proportions of correct and erroneous responses, and thus received an equivalent number of juice rewards during the two types of trials. The number of nonsaccadic movements, which included blinks and noise-related artifacts, was also similar in the saccade and fixation conditions [M1, movement (3.4 ± 2.6, mean ± SD nonsaccadic movements per block) versus fixation (2.6 ± 2.3), P = ns; M2, movement (2.4 ± 2.5) versus fixation (2.1 ± 2.4), P = ns]. Eye movements during saccade blocks typically had amplitudes between 4 and 9 deg, corresponding to the visual targets, whereas those observed on fixation blocks had amplitudes that were uniformly distributed (Fig. 2*C*).

Saccade-related Brain Activity

Figure 3*A* illustrates saccade-related activity superimposed over parasagittal and transverse cross-sections. Parasagittal cross-sections (Fig 3*A*, first row) show activation in medial occipital cortex (V1), posterior parietal cortex (LIP, PIP), superior temporal sulcus (MST), lateral frontal cortex (FEF), superior colliculus (sc) and posterior dorsal thalamus (pulv). Transverse cross-sections (Fig. 3*A*, second row) show the parietal, frontal and STS activations in more detail. These panels also highlight activations observed in several subcortical structures, including the superior colliculus and pulvinar.

In order to visualize the cortical activation pattern more clearly, the data were projected onto a reconstructed representation of the cortical surface and aligned to an atlas (Fig. 3*B*; see Materials and Methods for details). Inflated and flattened hemispheric views of the cerebral cortex show a large activation in lateral frontal cortex, several smaller activations in posterior parietal cortex, a swath of activation in the STS, and patchy activations in occipital and dorsomedial frontal cortex. On the flattened view of the left hemisphere (Fig. 3*B*, right panel), activations are shown relative to areal boundaries determined on the basis of cytoarchitectonic properties (Felleman and Van Essen, 1991) that were previously registered to the atlas.

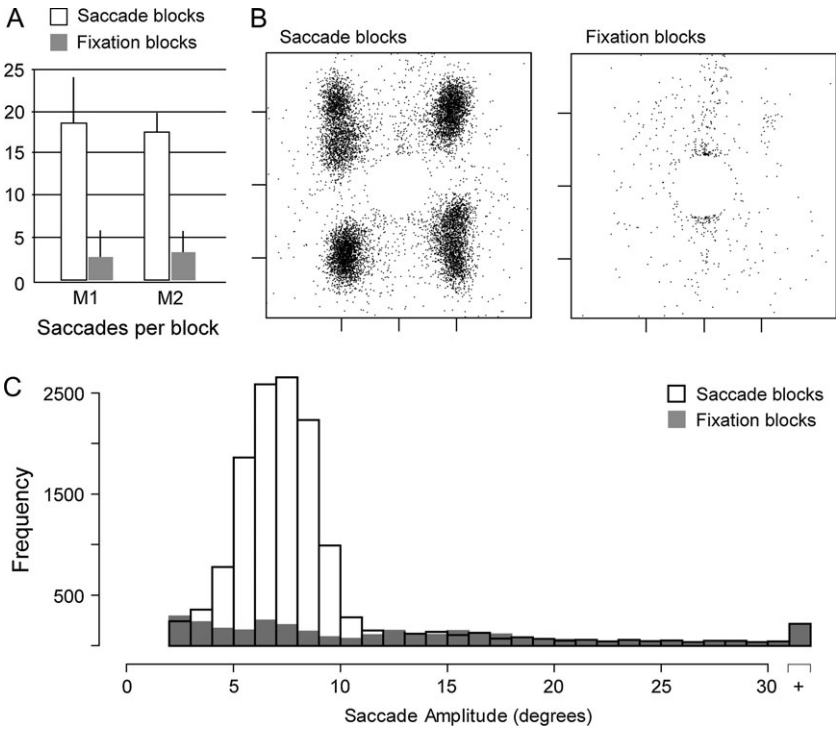

Figure 2. Behavioral summary. (*A*) Bar graph showing the mean number of saccades per saccade block (white bars) and fixation block (gray bars) for each of the two subjects, excluding artifacts. Error bars show standard deviations across blocks. (*B*) Scatterplots showing saccade endpoints for all trials from subject M1 (saccade trials, left; fixation trials, right), excluding artifacts. Tick marks on the horizontal and vertical axes indicate −5°, 0 and 5°. (*C*) Frequency histogram showing the amplitudes of all eye movements made during saccade blocks (white fill) and fixation blocks (gray fill) for subject M1.

According to the projected boundaries from the Felleman and Van Essen study, the lateral frontal activations were centered on FEF in both hemispheres, with spread into adjacent area 6 and posterior prefrontal cortex (area 45 and 46). The dorsomedial frontal activation was localized to a spot at the border between anterior SMA and posterior medial area 9, although this activation was present only in the right hemisphere (Fig. 3*B*, inflated view). While the Felleman and Van Essen study did not identify the location of the SEF, the location of this activation is consistent with previous reports of SEF relative to the gross anatomy (i.e. cingulate and arcuate sulci and the dorsomedial convexity). In posterior parietal cortex, the strongest activations were at a dorsal site on the lateral bank of the IPS and a more ventral site in caudal IPS. These two activation peaks were connected by active voxels that covered much of the lateral bank and parts of the medial bank. According to the Felleman and Van Essen boundaries, the peaks resided within the lateral and posterior intraparietal areas (LIP, PIP), respectively, with active voxels in VIP and parts of area 5 (on the opposing medial bank). Another activation was evident in posterior area 5 on the gyral surface, corresponding to the medial dorsal parietal area (MDP) near the borders with MIP and area PO. Small activations were also observed on the posterior bank of the lunate sulcus, corresponding to visual area V3A. A prominent activation near the gyral surface of the intraparietal lobule extended into caudal STS, as part of an activation spanning area 7a and the middle superior temporal area (MST). The remainder of active voxels in temporal cortex was found on the posterior bank and fundus of the superior temporal sulcus. This posterior-fundal activity spanned a larger than expected extent of the STS (nearly 20 mm), covering cortex consistent with the middle temporal area (MT), part of inferior MST (MSTi), the fundus of the superior temporal sulcus (FST), the superior temporal polysensory area (STP) and visual area V4 (primarily V4-temporal with spread into V4 proper). Additional cortical activations were also found in both striate (V1) and extrastriate visual cortex (V2, V3).

To summarize our findings at the group level, local maxima (peaks) in the activation map were identified along with regions of significant activity ($P < 0.05$) around each peak. A total of 31 saccade-related ROIs was identified in this fashion; one ROI was located in a fluid space (see Fig. 3*A*, second row, third column 'sinus') and therefore was discarded from consideration. The remaining thirty ROIs were located in thalamus, midbrain, and over the cerebral cortex (Fig. 3, Table 1). In several cases, the activation peak for a given ROI was located in one cortical area (as defined by projected borders; see Fig. 3*B*), but the collection of active voxels assigned to that ROI spanned multiple areas. For instance, the ROIs located within the middle of the intraparietal sulcus spanned both dorsal and ventral portions of the sulcus (corresponding to LIP and VIP, see Fig. 3*B*), and also showed some spread onto the opposing medial bank. This analysis is partly subjective, since smoothing and minimal peak separation parameters are somewhat arbitrary, chosen to yield a set of regions that reflects the experimenter's best sense of the data. With this caveat in mind, the table provides a reasonable summary of the number, sizes, and locations of saccade-related activations identified in the present study.

Individual Subject Statistical Maps

We next examined the distribution of saccade-related activations for consistency across hemispheres and individual subjects. In particular, we wished to establish the extent of each

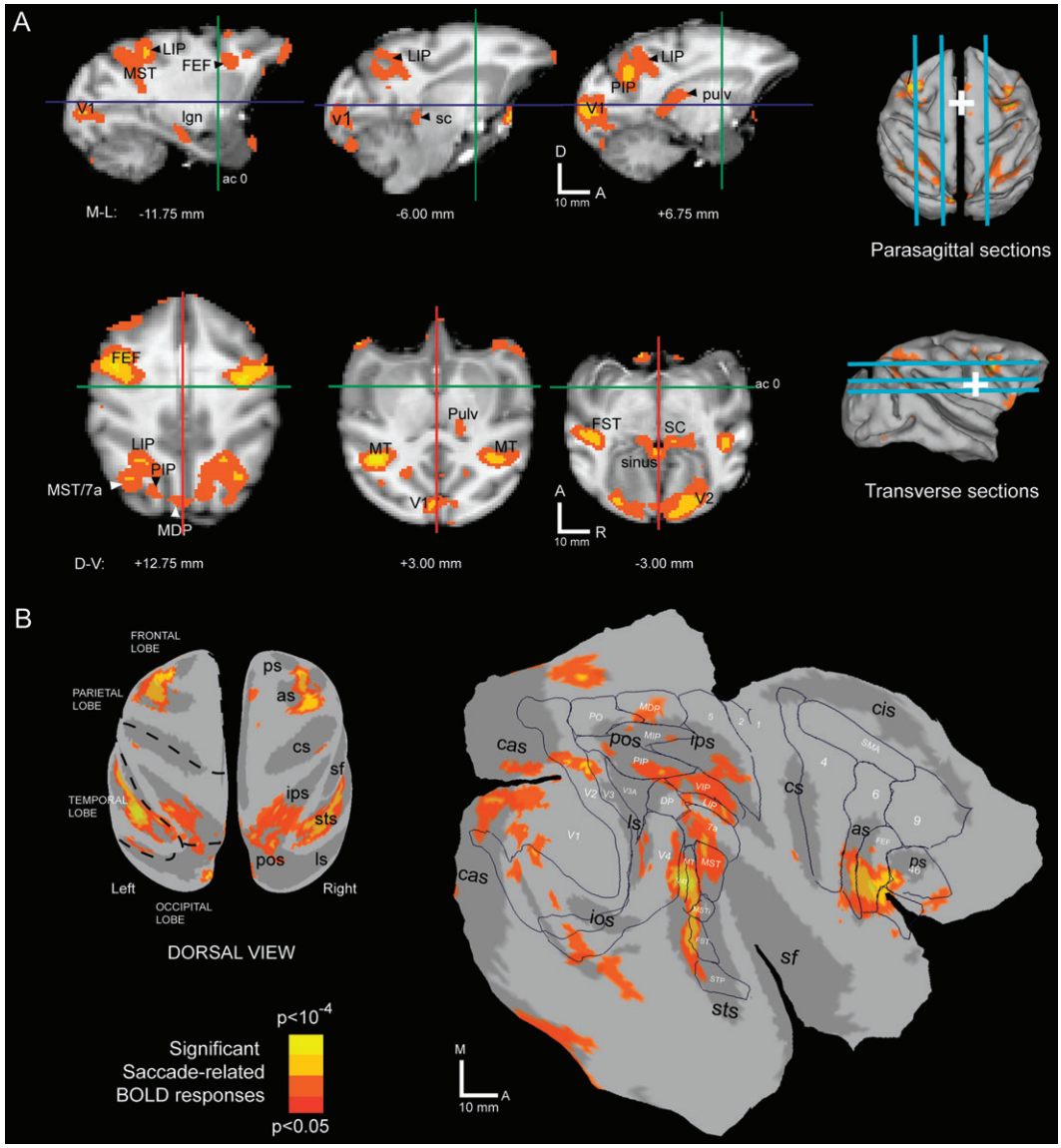

Figure 3. Saccade-related activations in the monkey. Brain sites significantly active ($P < 0.05$) during the saccade task are color-labeled (see color scale) and superimposed over (*A*) parasagittal (first row) and transverse (second row) cross-sections and (*B*) cortical surface renderings. In (*A*), slice positions are shown over dorsal and lateral view renderings of the cortical surface. Perpendicular lines (cross-sections) and white cross hairs (surface views) indicate the position of the anterior commissure. In (*B*), the same data set is shown after projection to the cortical surface of subject M1. See text for details.

activation and its location relative to anatomical landmarks. Four broad domains were examined: the frontal cortex (Fig. 4), the posterior parietal cortex (Fig. 5), the superior temporal sulcus (Fig. 6) and subcortical structures (Fig. 7). In many cases, the individual subject activations did not precisely match the group activation pattern (Fig. 3). This is due to both true variation in the anatomical substrates between the subjects as well as variation due to noise. The small size of the subject pool precluded a complete analysis of positional variation for each region. However, we were able to gauge intersubject variability relative to within subject variability by comparing data from the four hemispheres. In general, interhemispheric differences (i.e. within subject) were less than intersubject differences, which is consistent with the view that the macaque saccade system is bilaterally symmetric. This gave us confidence that differences in the two animals were due, at least in part, to true variations in their saccade-related neural substrates. In addition, viewing the data in this way helped to assess whether or not any hemispheric asymmetries were consistently present in both subjects.

Figure 4 shows saccade-related activity in the frontal cortex. A fixed-effects analysis was applied to each individual's data set. To compare data from the four hemispheres, the results were projected onto a representation of left and right hemispheres, and left hemisphere data were flipped across the vertical axis. As was the case in the group data set, individual subject frontal activation was divided between a large dorsolateral area and a small dorsomedial area. Dorsolaterally, all four panels show activation in the posterior third of the principal sulcus and on the anterior bank of the arcuate sulcus. For both subjects, frontal activation was similar in the two hemispheres (Fig. 4, compare upper and middle rows within each column). Between subjects, however, there were several notable differences.

Table 1
Macaque brain regions with visuo-oculomotor activity

ROI name[a]	Hem.	AC-PC coordinate (mm)			Volume (mm^3)	Peak *Z* value	Mean % change (SE)	
		ML	AP	DV			Subject M1	Subject M2
Frontal cortex								
FEF	L	−17.3	5.3	12.0	64.1	4.2	0.15 (0.07)	0.21 (0.04)
	R	16.5	2.3	11.3	57.4	3.9	0.26 (0.12)	0.21 (0.05)
SEF	R	1.5	6.0	17.3	3.4	2.1	0.26 (0.17)	0.12 (0.04)
Posterior parietal cortex								
LIP	L	−9.8	−20.3	9.8	30.4	2.8	0.21 (0.08)	0.13 (0.04)
	R	9.0	−18.8	9.8	47.3	2.9	0.20 (0.07)	0.11 (0.04)
	R	9.0	−23.3	13.5	20.3	2.4	0.17 (0.09)	0.13 (0.05)
PIP	L	−7.5	−25.5	7.5	37.1	2.4	0.23 (0.08)	0.10 (0.05)
	R	5.3	−25.5	8.3	54.0	3.0	0.28 (0.08)	0.12 (0.06)
Temporal cortex								
MST	L	14.3	−23.3	6.8	54.0	3.7	0.25 (0.10)	0.15 (0.05)
	R	−14.0	−24.0	10.5	47.3	2.8	0.34 (0.07)	0.11 (0.05)
MT	L	18.0	−20.3	1.5	43.9	3.1	0.34 (0.08)	0.19 (0.05)
	R	−17.3	−21.8	3.0	57.4	5.3	0.18 (0.06)	0.12 (0.04)
FST	L	−17.3	−18.0	−0.8	54.0	3.5	0.23 (0.08)	0.16 (0.05)
STP	L	−21.0	−15.0	−5.3	54.0	3.9	0.20 (0.07)	0.21 (0.04)
	L	−21.0	−11.3	−9.0	33.8	2.5	0.18 (0.08)	0.14 (0.04)
Occipital cortex								
V1	Mid	−0.8	−34.5	1.5	54.0	3.1	0.32 (0.11)	0.20 (0.09)
	Mid	−0.8	−37.5	−8.3	30.4	3.4	0.66 (0.16)	0.29 (0.19)
	L	−13.5	−34.5	−3.0	16.9	2.9	0.25 (0.10)	0.24 (0.07)
	L	−8.3	−37.5	−2.3	23.6	2.3	0.19 (0.13)	0.30 (0.08)
	R	9.8	−36.0	−2.3	60.8	4.0	0.27 (0.10)	0.29 (0.07)
	R	4.5	−38.3	−2.3	47.2	3.2	0.25 (0.16)	0.49 (0.09)
V2	L	−8.3	−33.0	−9.8	30.4	3.5	0.17 (0.09)	0.25 (0.07)
	R	2.3	−33.8	−8.3	43.9	2.8	0.18 (0.11)	0.27 (0.06)
	R	8.3	−33.0	−12.0	40.5	3.4	0.27 (0.10)	0.24 (0.07)
V3A	R	11.3	−29.3	8.3	16.9	2.6	0.33 (0.10)	0.17 (0.10)
V4	L	−18.0	−28.0	8.3	13.5	2.4	0.36 (0.35)	0.36 (0.17)
Subcortical structures								
SC	L	−4.5	−17.3	−3.0	16.9	2.6	0.27 (0.09)	0.09 (0.05)
	R	3.8	−17.3	−3.8	10.1	2.5	0.22 (0.07)	0.17 (0.05)
Pulv	R	6.8	−13.3	2.3	10.1	2.4	0.13 (0.07)	0.15 (0.04)
MD	L	−3.0	−6.8	0.0	3.4	2.1	0.19 (0.06)	0.10 (0.04)

[a]For cortical sites, 'ROI name' was based on the location of the peak voxel, projected to the cortical surface atlas and evaluated relative to boundaries from a published anatomical study (Felleman and Van Essen, 1991). For subcortical sites, 'ROI name' was based on an atlas containing subcortical anatomy (Paxinos *et al.*, 1999). Most active sites were spread across multiple regions. In some cases, more than one ROI occurred within a single area.

Activity behind the arcuate fundus in particular was substantially different in the two subjects. One subject (M1) showed a small amount of activity posterior to the arcuate fundus, while the other showed a large activation of postarcuate frontal cortex (areas 6 and 4). Inspection of the individual subject activation map over structural cortical anatomy (bottom row) confirmed that the postarcuate activation in subject M2 was not an artifact of the projection procedure. In particular, parasagittal cross-sections from M2 show posterior bank labeling separated from the anterior bank labeling by several millimeters (not shown), and a transverse section illustrates labeling in the arcuate spur and central sulcus (Fig. 4, bottom row, middle column). Similar cross-sections from subject M1 showed no evidence of extensive postarcuate activity, even when thresholds were lowered below the criterion level (not shown).

The discrepancy in postarcuate activation could be explained if subject M2 moved another effector (such as a limb or the jaw) differentially during the saccade and fixation trials. Even a small difference in skeletal movement during saccade and fixation blocks could have disproportionate effects on the resulting statistical images, since skeletal behaviors typically generate larger BOLD changes than eye movements (Astafiev *et al.*, 2003; Connolly *et al.*, 2003). Consistent with this explanation, subject M2 also showed a small but significant activation on the primary motor strip (anterior bank of the central sulcus, area 4) and in the superior parietal lobule (area 5). In humans, eye blinks have been hypothesized to produce atypical activations of frontal cortex near human FEF (Tehovnik *et al.*, 2000). However, there was no evidence for different numbers of blinks in the two animals. Also, the number of rewards received by the two subjects was similar in the saccade and fixation trials, thus ruling out an obvious cause for differential sucking or jaw movements. Other trivial explanations, such as differences in visual stimuli, behavior, coil position and scanning parameters, were also ruled out, since they were nearly identical in the two subjects. Neither animal made any appreciable head movements, since the head was bolted in place (see Fig. 1*A*). We cannot, however, rule out the possibility that subjects contracted the neck muscles in an attempt to move the head, and that subject M2 did this differentially during saccade blocks compared to fixation blocks.

Both of the subjects in the present study showed focal activation of dorsomedial frontal cortex, medial to the dorsalmost tip of the arcuate sulcus (Fig. 4, upper right corner of each flat map panel), a position consistent with that of SEF (Schlag and Schlag-Rey, 1985; Tehovnik *et al.*, 2000). In the group data, SEF activation was relatively weak and showed up only in the right hemisphere. A previous study (Koyama *et al.*, 2004) also found weak SEF activation at the group level, which the authors attributed to the simplicity of the task and the overtraining of the subjects. Our data suggest an alternative or additional factor.

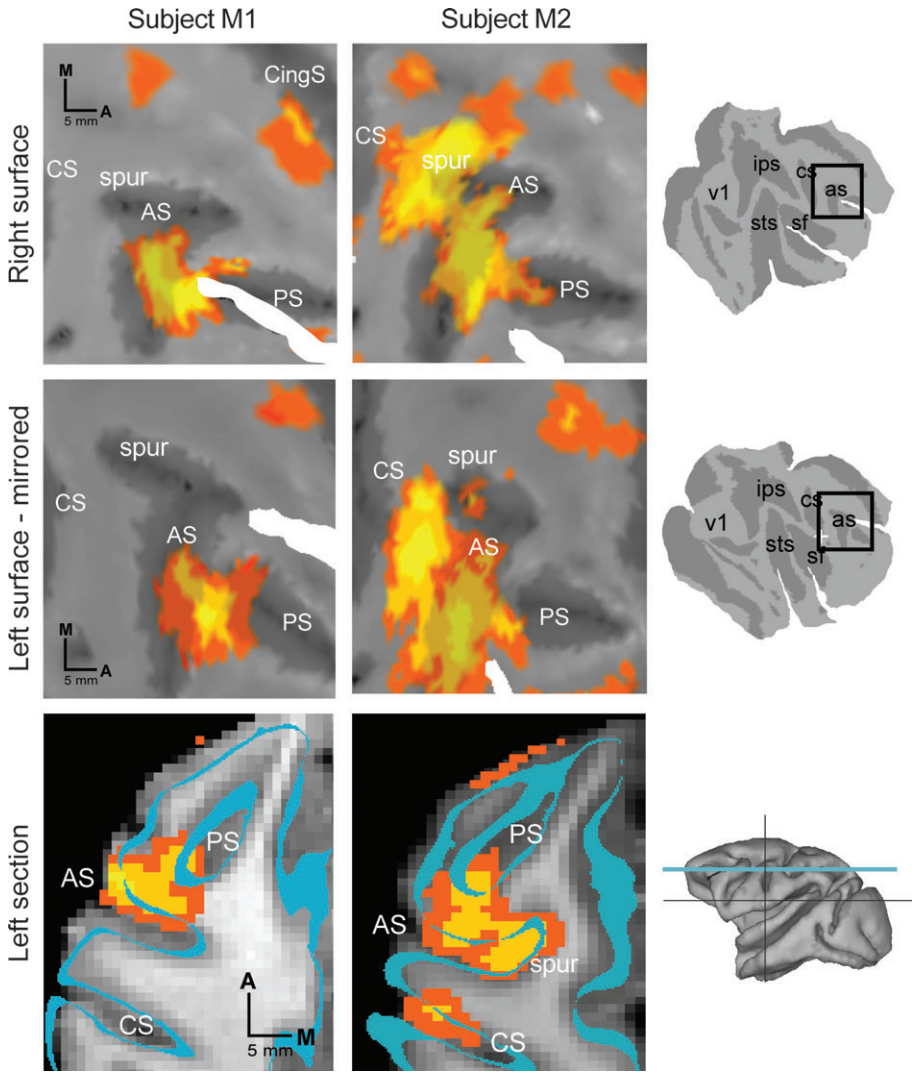

Figure 4. Frontal cortex summary. Frontal cortical activations ($P < 0.05$) from each subject (M1, first column; M2, second column) are color-coded for statistical significance (color scale as in Fig. 3) and superimposed on the corresponding flat maps (first and second rows) and cross-sections (third row) from that subject. In the first row, results from right frontal cortex are shown superimposed on a cropped portion of the cortical surface. In the second row, results from left frontal cortex are superimposed on a cropped portion of the left frontal cortical surface and mirrored across the horizontal axis. In the third row, representative transverse cross-sections through left frontal cortex taken from approximately the same level for each subject illustrate the pattern of arcuate labeling observed in the two subjects. The outline of the cortical surface used for data projection (see Materials and Methods) is indicated by the cyan bands. Cropping windows (first two rows, black boxes) and approximate slice plane (third row, cyan line) are indicated in the rightmost column. Scale bars are indicated separately for each row. Spur, arcuate spur. All other conventions as in Figure 3.

SEF activity at the individual subject level was at a slightly different position in each subject. This positional discrepancy, combined with the relatively small size of the SEF, may be a factor in poor SEF group activation.

Figure 5 shows saccade-related activity in the posterior parietal cortex. All four hemispheres showed an activation pattern dominated by inferior parietal lobular activation with some activation in the superior parietal lobule. In general, this pattern was consistent with published reports of saccade-related processing areas in the posterior parietal cortex. However, the parietal data were less similar across hemispheres than the frontal data, suggesting that either true interhemispheric differences exist in macaque parietal cortex or that, for some reason, our observations were less reliable in this part of the brain than in frontal cortex.

In all four hemispheres, activation was present on the lateral bank of the intraparietal sulcus. Weaker activation extended from this region down into the IPS fundus and a short distance up onto the gyrus of the inferior parietal lobule. The activations in the lateral bank and fundus of the IPS conform to the boundaries of LIP (as delineated by Felleman and Van Essen, 1991; Thier and Andersen, 1998) and VIP (Felleman and Van Essen, 1991), respectively. A more recent study defines separate cytoarchitectonic zones, called dorsal and ventral LIP (LIPd and LIPv), each of which extends further rostrally down the intraparietal sulcus than the LIP of the earlier studies (Lewis and Van Essen, 2000). In the group data, activation occurred within both LIPv and LIPd but was confined to only the posterior two-thirds of their rostro-caudal extent. In general, activity in the lateral bank trended toward more dorsal activation anteriorly and more ventral activation posteriorly.

The group analysis revealed an activation in PIP, which was posterior, inferior and medial to LIP (see Fig. 3). While this region was significantly active in both hemispheres of both subjects, the PIP-centered peak was separable from the LIP-centered peak in only two of four hemispheres (left hemisphere

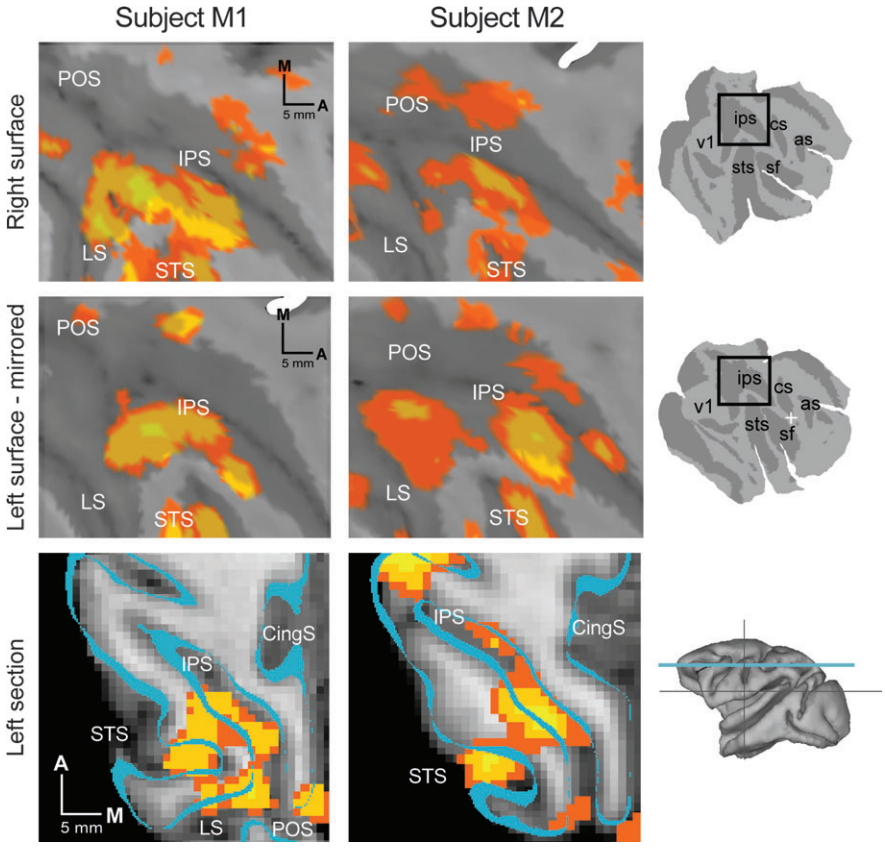

Figure 5. Parietal cortex summary. All conventions as in Figure 4. See text for details.

in both subjects). While it is intriguing to speculate that this result could represent a parietal hemispheric asymmetry, the between-subject difference was at least as different as the interhemispheric difference, making this interpretation unlikely. Recently, the caudal portion of the intraparietal sulcus has been shown to be activated during the viewing of 3-D scenes (Taira *et al.*, 2000; Tsutsui *et al.*, 2003; Tsao *et al.*, 2003), as well as during reaching movements to visual targets (Calton *et al.*, 2002), and weakly activated during the planning and execution of saccades (Snyder *et al.*, 1997, 2000).

An additional parietal region was active lateral to the PIP site on the anterior bank of the lunate sulcus. This region is consistent with area V3A (Felleman and Van Essen, 1991) and was active in three out of four hemispheres.

Individual hemispheres showed activation on the superior parietal lobule (SPL, area 5), but none of these activations survived the group analysis. All four hemispheres were active in a region slightly posterior to LIP on the opposite side of the IPS. In three out of four hemispheres, this activation was on the dorsal surface of the SPL at a location consistent with the medial dorsal parietal area (MDP). In the fourth hemisphere, a similar activation was present in the IPS at a location consistent with the medial intraparietal area (MIP). Most activity on the medial bank of the IPS could be explained as spread from activity on the lateral bank. Subject M2 showed the only exception to this, with convincing medial bank activation anterior to the other parietal activations. This site, which was located near the anterior intraparietal area (AIP), was active only in this subject's left hemisphere (Fig. 5, middle column, second and third rows).

On the medial aspect of the parietal lobe, only one of four hemispheres (Fig. 5, first column, first row, upper right) showed significant activation. This activation was situated near the caudal end of the cingulate sulcus, consistent with the medial parietal area (MP; Thier and Andersen, 1998). In the other three hemispheres, activation at this site did not exceed the statistical criterion, although medial wall activity was evident when the data were examined at lower thresholds (not shown).

Figure 6 shows the results for superior temporal cortex. Parasagittal cross-sections and a flat map from one hemisphere (M2, left) illustrate the characteristic activation pattern that was observed. The anterior bank of STS was active for the caudalmost 1–2 cm (Fig. 6, a). Rostral to this, the sulcus angles forward and activation was confined to the posterior-ventral bank and the fundus, which forms an invaginated third bank between the anterior-dorsal and posterior-ventral banks. The STS activation extended rostrally to slightly different positions in each hemisphere. As illustrated in the figure, both subjects showed evidence for clusters of activation distributed within the STS (Fig. 6, a–d). Robust activation of the 'motion complex' was unexpected, but can best be explained as the combined effects of peripheral visual transients and/or visual motion induced on the retina by the saccades. Saccades indirectly lead to activation of some neurons in areas MT and MST (Thiele *et al.*, 2002). Thus, it is reasonable to infer that eye velocities were achieved that would drive many of the velocity-tuned motion-sensitive cells in MT, MST and possibly even FST.

Figure 7 shows subcortical saccade-related activations in the two subjects. The superior colliculus was activated bilaterally in both subjects (Fig. 7*A*). In subject M1, the left and right parts of

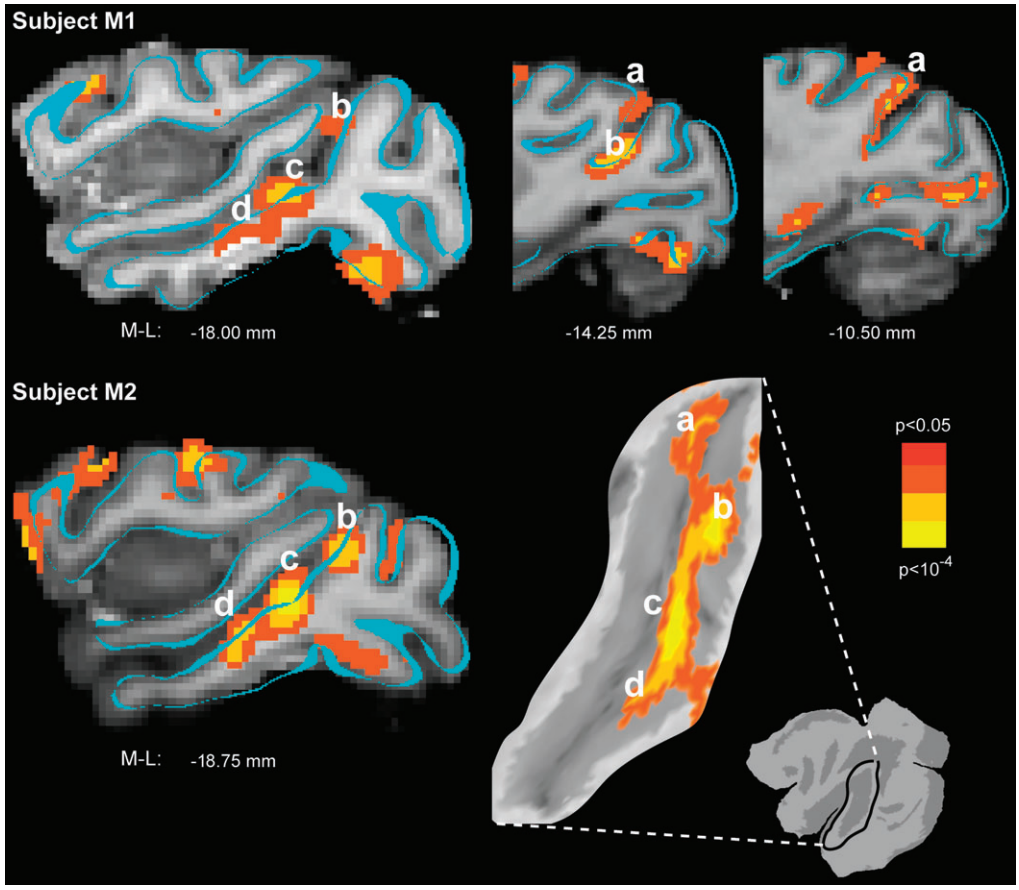

Figure 6. Temporal cortex summary. Superior temporal activation ($P < 0.05$) from each subject (M1, first row; M2, second row) is color-coded for statistical significance and superimposed on the corresponding anatomical images from that subject. Parasagittal cross-sections show the activation pattern that was characteristically observed along the superior temporal sulcus, including a caudal anterior bank site (a) and several additional sites on the posterior bank and fundus (b–d). For subject M2, results are also shown projected and superimposed onto a cropped, flattened portion of the left superior temporal sulcus for reference.

the active cluster were coextensive; in M2, distinct clusters of active voxels were observed 1–2 mm off the midline on either side (not shown).

Several thalamic activations were observed. A unilateral activation in right dorsal posterior thalamus, consistent with the lateral pulvinar nucleus, was present in both subjects (Fig. 7*B*,*D*). Inspection of the individual statistical maps at lower thresholds ($P < 0.10$) provided no evidence of left pulvinar activation in either subject (data not shown). A ventral posterior thalamic activation was observed in both subjects (Fig. 7*C*), consistent with the location of the lateral geniculate nuclei (LGN). At the statistical criterion chosen for this study ($P < 0.05$), the LGN activity was bilateral in one subject but occurred only on the right in the other subject (Fig. 7*D*). This discrepancy between the two subjects may have been due to insufficient statistical power, since by lowering the threshold ($P < 0.10$) we found evidence for left LGN activity in both subjects (data not shown). In the central thalamus, at a location consistent with the medial dorsal nucleus (Fig. 7*E*), only a single voxel survived the group analysis as a saccade-related ROI (not shown; see Table 1). However, at lower statistical thresholds, the central thalamic activation was bilateral in both subjects.

Neither the cerebellum, basal ganglia nor brainstem were activated in the present experiment, even at lowered statistical threshold. Since numerous neuronal recording studies have reported saccade-related activity in these structures, we suspect that a combination of the small size of these areas, the positioning of the surface coil above the skull, and the distorting effects of body and neck movements on the lower brain structures all contributed to a low signal-to-noise ratio in these parts of the brain.

Discussion

The oculomotor system is composed of a distributed network of brain areas in the cerebral cortex, thalamus, midbrain, cerebellum and brainstem. The current study was designed to detect changes in blood oxygen level, and to compare the anatomical distribution of this metabolic marker of neuronal activity with the patterns of activation previously determined using extracellular recordings of action potentials (Logothetis, 2002). Most of the active sites revealed by the BOLD signal were expected on the basis of the single unit literature, including LIP, FEF, SEF and several visual processing areas. There were a few unexpected findings, including unilateral activation of the pulvinar, and extensive activation within the STS.

Frontal Cortex

Single neuron recording in monkeys and imaging work in humans has revealed two areas activated by saccades in frontal cortex: FEF, in the dorsolateral frontal cortex, and SEF, in the dorsomedial frontal cortex (Tehovnik *et al.*, 2000). FEF was first

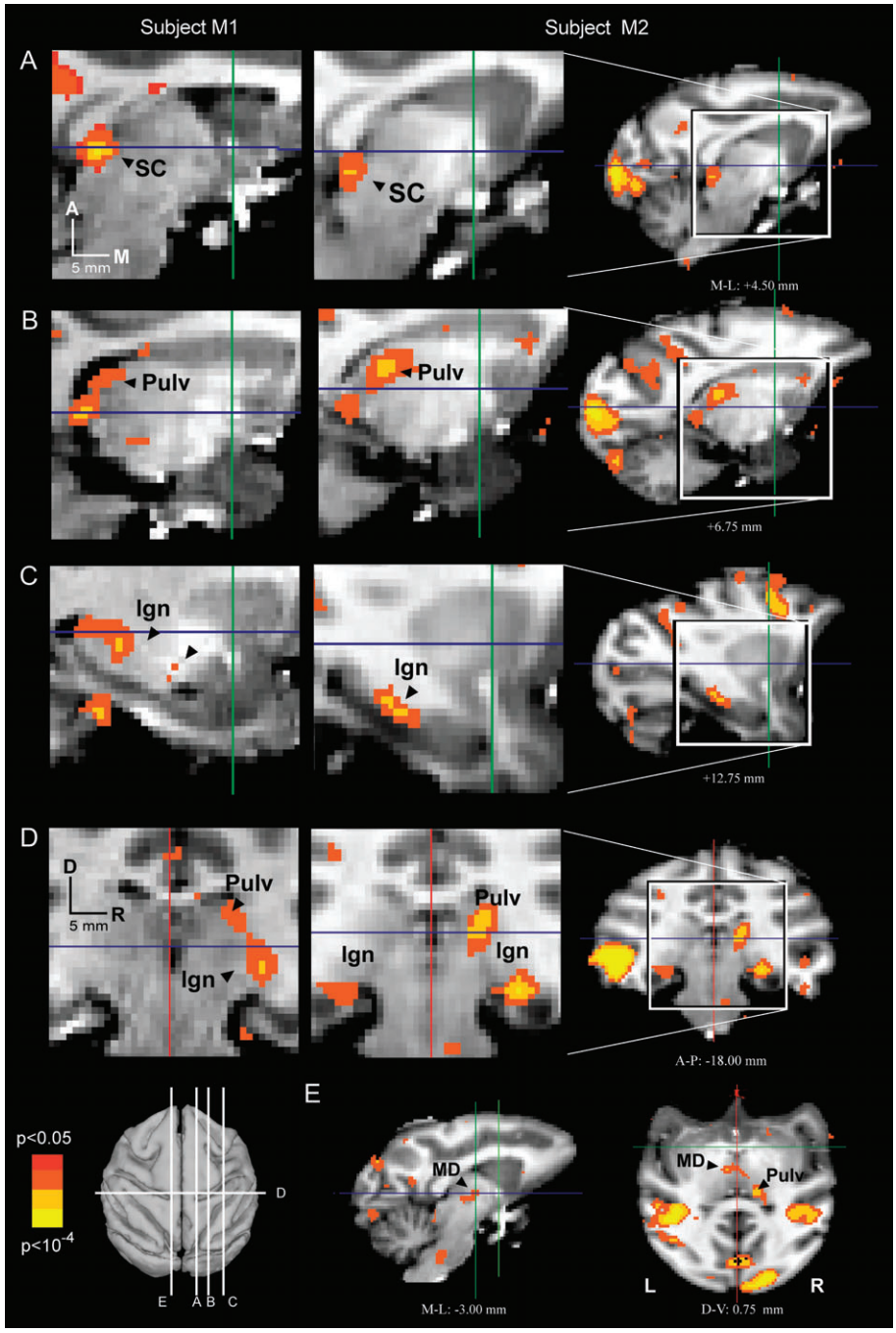

Figure 7. Subcortical summary. Subcortical activations ($P < 0.05$) from each subject (M1, first column; M2, second column) are color-coded for statistical significance and superimposed on the corresponding anatomical images from that subject. Note that coronal and transverse sections (panels *D* and *E*) use the neurological convention, with the right side of the illustrations representing the right side of the subject. Coordinates and magnitudes of activations that survived the group analysis appear in Table 1.

described by Ferrier (1876), who evoked conjugate, contraversive saccadic eye movements by stimulating lateral frontal cortex. Subsequent workers refined Ferrier's initial observation by mapping a zone on the anterior bank of the arcuate sulcus where saccades can be evoked using low currents (10–50 μA), and by demonstrating direct connections from this region to the superior colliculus and several other brainstem nuclei (Robinson and Fuchs, 1969; Bruce *et al.*, 1985; Stanton *et al.*, 1988; Moschovakis *et al.*, 2004; Koyama *et al.*, 2004). This region was clearly activated in our fMRI study. The location and the extent of activity matches the location and extent of FEF, as determined by functional and anatomical studies (Felleman and Van Essen, 1991; Bruce *et al.*, 1985; Moschovakis *et al.*, 2004).

Unlike FEF, the second major saccade-related region in the frontal cortex, SEF (Schlag and Schlag-Rey, 1985, 1987), appears to be recruited primarily in connection with relatively complex or cognitively challenging saccade tasks (Olson and Gettner, 1995; Chen and Wise, 1995; Amador *et al.*, 2004). The present findings were consistent with this functional distinction, with much greater FEF activation than SEF activation.

In one of our two animals we observed activation posterior to FEF, in the postarcuate cortex (Brodmann's area 6). While this area has traditionally been associated with visually guided skeletomotor behavior, recent evidence suggests an oculomotor role for the rostral portion of area 6, perhaps in addition to its traditional skeletomotor role. Moschovakis *et al.* (2004) showed saccade-related activity in rostral area 6 by comparing glucose utilization (using the 2-deoxyglucose method) across the frontal cortices of subjects who had performed tasks with different saccadic requirements. This study also provided supporting neuroanatomical evidence for an area 6 oculomotor function by tracing multisynaptic retrograde connections from the extraocular muscles back to rostral area 6. Koyama *et al.* (2004) found activity behind the arcuate sulcus in approximately the same location as the Moschovakis study using BOLD fMRI. Our finding of primary motor cortex activation along with area 6 activation is consistent with the idea that the area 6 activation reflects an associated somatomotor behavior, but no firm conclusion can be drawn at this time.

Saccade-related activation in the posterior principle sulcus is also not a new finding, having been reported in many single-unit electrophysiology studies (e.g. Funahashi *et al.*, 1990, 1991; Takeda and Funahashi, 2002). Those experiments demonstrated that the saccade-related activity in dorsolateral prefrontal cortex resembled that found in FEF proper with two exceptions: low current (<50 μA) microstimulation there does not evoke regular eye movements, and neurons with noncanonical eye movement related responses are often found comingled with saccade-related neurons in the more anterior frontal area. The current study reaffirms the notion that the frontal eye movement system covers a fairly large region of frontal cortex and may be comprised of multiple cortical areas with different oculomotor roles.

Posterior Parietal Cortex

Single neuron recording has revealed prominent visual and saccade-related activity in much of the inferior parietal lobule (Brodmann's area 7), including areas 7a and LIP (visual and oculomotor activity) and VIP, cIPS and AIP (visual activity). Oculomotor responses are most prominent in area LIP, a cytoarchitectonically distinct zone located in the posterior half of the intraparietal sulcus (Barash *et al.*, 1991; Felleman and Van Essen, 1991; Snyder *et al.*, 1996; Goldberg *et al.*, 2002; Roitman and Shadlen, 2002; Dorris and Glimcher, 2004). Area 7a, located adjacent to LIP on the dorsal surface of the inferior parietal lobule, has weaker visual responses than LIP and tends to respond after saccades rather than before them (Barash *et al.*, 1991). In contrast to the inferior parietal lobule, the superior lobule has a skeletomotor bias (Mountcastle *et al.*, 1975; Johnson *et al.*, 1996; Battaglia-Mayer *et al.*, 2001; Eskandar and Assad, 2002) and somewhat weaker visual responses than the inferior lobule (Kalaska and Crammond, 1995; Colby and Duhamel, 1996), although some superior parietal areas also respond during saccades (Battaglia-Mayer *et al.*, 2001).

Based on these single neuron recording results, we expected prominent activity in LIP, moderate activity in the remainder of the inferior parietal lobule, and possibly some scattered weak foci in the superior parietal lobule. In fact, we found three distinct regions of activation. First, prominent activity was seen in a wide swath of cortex covering most of LIP and VIP and extending up onto a portion of area 7a. This is consistent with previous single neuron data, although we did not anticipate that the 7a activation would be only partial. The second focus of activity was posterior and inferior to the first, located at the junction of the IP and lunate sulci, and represented PIP or possibly the dorsal parietal (DP) area (Felleman and Van Essen, 1991). Finally, a third, smaller region of activation was found near the lip of the medial bank of the IPS at a location just posterior to that of LIP. This region straddled the IP sulcus and adjacent gyrus in M2, but lay completely on the gyrus in M1.

Subcortical Structures

The subcortical activations we observed (medial dorsal, pulvinar and lateral geniculate thalamic nuclei and the SC) are consistent with single neuron recording data. Medial dorsal and 'paralaminar' nuclei connect to both the superior colliculus and the frontal oculomotor areas, and appear to relay important saccade-related signals from the colliculus to the cortex (Sommer and Wurtz, 2004; Tanibuchi and Goldman-Rakic, 2005). The medial and lateral pulvinar provide a similar pathway between the colliculus and the inferior parietal lobule (Asanuma *et al.*, 1985; Hardy and Lynch, 1992), and may serve an analogous feedback role for the parietal oculomotor areas (Robinson, 1993). An unexpected finding was the presence of unilateral pulvinar activation. This is potentially significant because it could be evidence of hemispheric asymmetry in the macaque orienting system. Right unilateral pulvinar activation has been reported in a PET study of the human attentional system (Corbetta *et al.*, 1991), and the right pulvinar may be selectively damaged in individuals with schizophrenia (Highley *et al.*, 2003). The relationship between these results in humans and the present findings will require further study.

The LGN are not usually considered in an oculomotor context, but like V1 their activation is expected in a task involving peripheral visible targets. Moreover, the LGN may have specific roles related to oculomotor processing, including suppression of visual processing during saccade execution (Martinez-Conde *et al.*, 2002; Reppas *et al.*, 2002; Sylvester *et al.*, 2005). To our knowledge, the present study represents the first published report of BOLD activity in the LGN of awake behaving monkeys, although a previous study reported BOLD activity in the LGN of anesthetized animals (Logothetis *et al.*, 1999).

Cortical and Subcortical Saccade Control in Humans and Monkeys

Visually guided eye movements are conserved at the behavioral level in humans and monkeys, making oculomotor paradigms ideal for comparing brain organization in the two species. The peripheral visual and oculomotor apparatuses are nearly identical across the two species. Subcortical structures are anatomically similar, although less is known about function. In the cerebral cortex, the frontal and posterior parietal cortices are greatly expanded in humans compared to macaques. Despite this expansion, the pattern of cortical activation observed when monkeys and humans make saccades is broadly similar (Koyama *et al.*, 2004). However, much remains unknown about the precise correspondence of cortical areas in the two species (Tehovnik *et al.*, 2000; Munoz, 2002).

In humans, frontal activity during saccades is spread over several anatomical areas (Beauchamp *et al.*, 2001; Astafiev *et al.*, 2003; see also Tehovnik *et al.*, 2000), including Brodmann's

areas 6 and 8, although several individual foci have yet to be differentiated. A dorsomedial area has been shown to exhibit similar functional properties as macaque SEF (Brooks-Eidelberg and Adler, 1992; Everling *et al.*, 1997; Petit and Haxby, 1999; Beauchamp *et al.*, 2001; Petit and Beauchamp, 2003; Yamamoto *et al.*, 2004), with responses during eye movement tasks that scale roughly with task difficulty.

In posterior parietal cortex, a simple saccade task activates up to four distinct sites in humans (Corbetta *et al.*, 1998), distributed mostly medial to the intraparietal sulcus. In humans, the inferior parietal lobule does not typically show saccade-related activity, and yet some of the active parietal areas in the superior parietal lobule exhibit similar functional properties as macaque inferior parietal areas. For instance, one human region in particular has been associated with macaque LIP on the basis of spatial selectivity, sustained activity during a memory period and oculomotor bias (Petit and Haxby, 1999; Sereno *et al.*, 2001; Connolly *et al.*, 2003; Medendorp *et al.*, 2003; Merriam *et al.*, 2003). Yet arguing for interspecies homologies based on these simple properties may be premature. Macaque LIP is known, for example, to represent not just the location but also the value of a visual stimulus (Dorris and Glimcher, 2004), and may represent other, more complex properties as well (Roitman and Shadlen, 2002). It will therefore be necessary to test for these additional properties in humans before coming to firm conclusions regarding homology.

Notes

We would like to thank Roger Tootell and Wim VanDuffel for help in developing the experimental setup, Tom Conturo for help with image acquisition, and Avi Snyder, Gordon Shulman, and David Van Essen for help with image analysis. This work was generously supported by the McDonnell Center for Higher Brain Function, the NIH (NEI, NRSA, and Washington University Conte Center) and the EJLB foundation.

Address correspondence to Justin T. Baker, Department of Anatomy & Neurobiology, Campus Box 8108, Washington University School of Medicine, St Louis, MO 63116, USA. Email: justin@eye-hand.wustl.edu.

References

Amador N, Schlag-Rey M, Schlag J (2004) Primate antisaccade. II. Supplementary eye field neuronal activity predicts correct performance. J Neurophysiol 91:1672–1689.

Asanuma C, Andersen RA, Cowan WM (1985) The thalamic relations of the caudal inferior parietal lobule and the lateral prefrontal cortex in monkeys: divergent cortical projections from cell clusters in the medial pulvinar nucleus. J Comp Neurol 241:357–381.

Astafiev SV, Shulman GL, Stanley CM, Snyder AZ, Van Essen DC, Corbetta M (2003) Functional organization of human intraparietal and frontal cortex for attending, looking, and pointing. J Neurosci 23:4689–4699.

Barash S, Bracewell RM, Fogassi L, Gnadt JW, Andersen RA (1991) Saccade-related activity in the lateral intraparietal area. I. Temporal properties; comparison with area 7a. J Neurophysiol 66:1095–1108.

Battaglia-Mayer A, Ferraina S, Genovesio A, Marconi B, Squatrito S, Molinari M, Lacquaniti F, Caminiti R (2001) Eye-hand coordination during reaching. II. An analysis of the relationships between visuomanual signals in parietal cortex and parieto-frontal association projections. Cereb Cortex 11:528–544.

Beauchamp MS, Petit L, Ellmore TM, Ingeholm J, Haxby JV (2001) A parametric fMRI study of overt and covert shifts of visuospatial attention. Neuroimage 14:310–321.

Boynton GM, Engel SA, Glover GH, Heeger DJ (1996) Linear systems analysis of functional magnetic resonance imaging in human V1. J Neurosci 16:4207–4221.

Brooks-Eidelberg BA, Adler G (1992) A frontal cortical potential associated with saccades in humans. Exp Brain Res 89:441–446.

Bruce CJ, Goldberg ME, Bushnell MC, Stanton GB (1985) Primate frontal eye fields. II. Physiological and anatomical correlates of electrically evoked eye movements. J Neurophysiol 54:714–734.

Calton JL, Dickinson AR, Snyder LH (2002) Non-spatial, motor-specific activation in posterior parietal cortex. Nat Neurosci 5:580–588.

Chen LL, Wise SP (1995) Supplementary eye field contrasted with the frontal eye field during acquisition of conditional oculomotor associations. J Neurophysiol 73:1122–1134.

Colby CL, Duhamel JR (1996) Spatial representations for action in parietal cortex. Brain Res Cogn Brain Res 5:105–115.

Connolly JD, Andersen RA, Goodale MA (2003) FMRI evidence for a 'parietal reach region' in the human brain. Exp Brain Res 153:140–145.

Corbetta M, Miezin FM, Dobmeyer S, Shulman GL, Petersen SE (1991) Selective and divided attention during visual discriminations of shape, color, and speed: functional anatomy by positron emission tomography. J Neurosci 11:2383–2402.

Corbetta M, Akbudak E, Conturo TE, Snyder AZ, Ollinger JM, Drury HA, Linenweber MR, Petersen SE, Raichle ME, Van Essen DC, Shulman GL (1998) A common network of functional areas for attention and eye movements. Neuron 21:761–773.

Denys K, Vanduffel W, Fize D, Nelissen K, Peuskens H, Van Essen D, Orban GA (2004) The processing of visual shape in the cerebral cortex of human and nonhuman primates: a functional magnetic resonance imaging study. J Neurosci 24:2551–2565.

Dorris MC, Glimcher PW (2004) Activity in posterior parietal cortex is correlated with the relative subjective desirability of action. Neuron 44:365–378.

Eskandar EN, Assad JA (2002) Distinct nature of directional signals among parietal cortical areas during visual guidance. J Neurophysiol 88:1777–1790.

Everling S, Krap.p.m.ann P, Flohr H (1997) Cortical potentials preceding pro- and antisaccades in man. Electroencephalogr Clin Neurophysiol 102:356–362.

Felleman DJ, Van Essen DC (1991) Distributed hierarchical processing in the primate cerebral cortex. Cereb Cortex 1:1–47.

Ferrier D (1876) The Functions of the Brain. London: Smith, Elder and Co.

Friston KJ, Holmes AP, Poline JB, Grasby PJ, Williams SC, Frackowiak RS, Turner R (1995) Analysis of fMRI time-series revisited. Neuroimage 2:45–53.

Funahashi S, Bruce CJ, Goldman-Rakic PS (1990) Visuospatial coding in primate prefrontal neurons revealed by oculomotor paradigms. J Neurophysiol 63:814–831.

Funahashi S, Bruce CJ, Goldman-Rakic PS (1991) Neuronal activity related to saccadic eye movements in the monkey's dorsolateral prefrontal cortex. J Neurophysiol 65:1464–1483.

Goldberg ME, Bisley J, Powell KD, Gottlieb J, Kusunoki M (2002) The role of the lateral intraparietal area of the monkey in the generation of saccades and visuospatial attention. Ann N Y Acad Sci 956:205–215.

Hardy SG, Lynch JC (1992) The spatial distribution of pulvinar neurons that project to two subregions of the inferior parietal lobule in the macaque. Cereb Cortex 2:217–230.

Highley JR, Walker MA, Crow TJ, Esiri MM, Harrison PJ (2003) Low medial and lateral right pulvinar volumes in schizophrenia: a post-mortem study. Am J Psychiatry 160:1177–1179.

Johnson PB, Ferraina S, Bianchi L, Caminiti R (1996) Cortical networks for visual reaching: physiological and anatomical organization of frontal and parietal lobe arm regions. Cereb Cortex 6:102–119.

Kalaska JF, Crammond DJ (1995) Deciding not to GO: neuronal correlates of response selection in a GO/NOGO task in primate premotor and parietal cortex. Cereb Cortex 5:410–428.

Koyama M, Hasegawa I, Osada T, Adachi Y, Nakahara K, Miyashita Y (2004) Functional magnetic resonance imaging of macaque monkeys performing visually guided saccade tasks: comparison of cortical eye fields with humans. Neuron 41:795–807.

Lewis JW, Van Essen DC (2000) Mapping of architectonic subdivisions in the macaque monkey, with emphasis on parieto-occipital cortex. J Comp Neurol 428:79–111.

Logothetis NK (2002) The neural basis of the blood-oxygen-level-dependent functional magnetic resonance imaging signal. Philos Trans R Soc Lond B Biol Sci 357:1003–1037.
Logothetis NK, Guggenberger H, Peled S, Pauls J (1999) Functional imaging of the monkey brain. Nat Neurosci 2:555–562.
Martinez-Conde S, Macknik SL, Hubel DH (2002) The function of bursts of spikes during visual fixation in the awake primate lateral geniculate nucleus and primary visual cortex. Proc Natl Acad Sci USA 99:13920–13925.
Medendorp WP, Goltz HC, Vilis T, Crawford JD (2003) Gaze-centered updating of visual space in human parietal cortex. J Neurosci 23:6209–6214.
Merriam EP, Genovese CR, Colby CL (2003) Spatial updating in human parietal cortex. Neuron 39:361–373.
Mintun MA, Fox PT, Raichle ME (1989) A highly accurate method of localizing regions of neuronal activation in the human brain with positron emission tomography. J Cereb Blood Flow Metab 9:96–103.
Moschovakis AK, Gregoriou GG, Ugolini G, Doldan M, Graf W, Guldin W, Hadjidimitrakis K, Savaki HE (2003) Oculomotor areas of the primate frontal lobes: a transneuronal transfer of rabies virus and [14C]-2-deoxyglucose functional imaging study. J Neurosci 24:5726–5740.
Mountcastle VB, Lynch JC, Georgopoulos A, Sakata H, Acuna C (1975) Posterior parietal association cortex of the monkey: command functions for operations within extrapersonal space. J Neurophysiol 38:871–908.
Munoz DP (2002) Commentary: saccadic eye movements: overview of neural circuitry. Prog Brain Res 140:89–96.
Nakahara K, Hayashi T, Konishi S, Miyashita Y (2002) Functional MRI of macaque monkeys performing a cognitive set-shifting task. Science 295:1532–1536.
Ojemann JG, Akbudak E, Snyder AZ, McKinstry RC, Raichle ME, Conturo TE (1997) Anatomic localization and quantitative analysis of gradient refocused echo-planar fMRI susceptibility artifacts. Neuroimage 6:156–167.
Ollinger JM, Corbetta M, Shulman GL (2001) Separating processes within a trial in event-related functional MRI. Neuroimage 13:218–229.
Olson CR, Gettner SN (1995) Object-centered direction selectivity in the macaque supplementary eye field. Science 269:985–988.
Paxinos G, Huang X-F, Toga AW (1999) The rhesus monkey brain in stereotaxic coordinates. New York: Academic Press.
Petit L, Beauchamp MS (2003) Neural basis of visually guided head movements studied with fMRI. J Neurophysiol 89:2516–2527.
Petit L, Haxby JV (1999) Functional anatomy of pursuit eye movements in humans as revealed by fMRI. J Neurophysiol 82:463–471.
Pinsk MA, Desimone K, Moore T, Gross CG, Kastner S (2005) Representations of faces and body parts in macaque temporal cortex: A functional MRI study. Proc Natl Acad Sci USA 102:6996–7001.
Reppas JB, Usrey WM, Reid RC (2002) Saccadic eye movements modulate visual responses in the lateral geniculate nucleus. Neuron 35:961–974.
Robinson DA, Fuchs AF (1969) Eye movements evoked by stimulation of frontal eye fields. J Neurophysiol 32:637–648.
Robinson DL (1993) Functional contributions of the primate pulvinar. Prog Brain Res 95:371–380.
Roitman JD, Shadlen MN (2002) Response of neurons in the lateral intraparietal area during a combined visual discrimination reaction time task. J Neurosci 22:9475–9489.
Schlag J, Schlag-Rey M (1985) Unit activity related to spontaneous saccades in frontal dorsomedial cortex of monkey. Exp Brain Res 58:208–211.
Schlag J, Schlag-Rey M (1987) Evidence for a supplementary eye field. J Neurophysiol 57:179–200.
Sereno MI, Pitzalis S, Martinez A (2001) Mapping of contralateral space in retinotopic coordinates by a parietal cortical area in humans. Science 294:1350–1354.
Snyder LH, Batista AP, Andersen RA (1997) Coding of intention in the posterior parietal cortex. Nature 386:167–170.
Snyder LH, Batista AP, Andersen RA (2000) Saccade-related activity in the parietal reach region. J Neurophysiol 83:1099–1102.
Sommer MA, Wurtz RH (2004) What the brain stem tells the frontal cortex. I. Oculomotor signals sent from superior colliculus to frontal eye field via mediodorsal thalamus. J Neurophysiol 91:1381–402.
Stanton GB, Goldberg ME, Bruce CJ (1988) Frontal eye field efferents in the macaque monkey. II. Topography of terminal fields in midbrain and pons. J Comp Neurol 271:493–506.
Sylvester R, Haynes JD, Rees G (2005) Saccades differentially modulate human LGN and V1 responses in the presence and absence of visual stimulation. Curr Biol 15:37–41.
Takeda K, Funahashi S (2002) Prefrontal task-related activity representing visual cue location or saccade direction in spatial working memory tasks. J Neurophysiol 87:567–588.
Taira M, Tsutsui KI, Jiang M, Yara K, Sakata H (2000) Parietal neurons represent surface orientation from the gradient of binocular disparity. J Neurophysiol 83:3140–3146.
Tanibuchi I, Goldman-Rakic PS (2005) Comparison of oculomotor neuronal activity in paralaminar and mediodorsal thalamus in the rhesus monkey. J Neurophysiol 93:614–619.
Tehovnik EJ, Sommer MA, Chou IH, Slocum WM, Schiller PH (2000) Eye fields in the frontal lobes of primates. Brain Res Brain Res Rev 32:413–448.
Thiele A, Henning P, Kubischik M, Hoffmann KP (2002) Neural mechanisms of saccadic suppression. Science 295:2460–2462.
Thier P, Andersen RA (1998) Electrical microstimulation distinguishes distinct saccade-related areas in the posterior parietal cortex. J Neurophysiol 80:1713–1735.
Tsao DY, Vanduffel W, Sasaki Y, Fize D, Knutsen TA, Mandeville JB, Wald LL, Dale AM, Rosen BR, Van Essen DC, Livingstone MS, Orban GA, Tootell RB (2003) Stereopsis activates V3A and caudal intraparietal areas in macaques and humans. Neuron 39:555–568.
Tsutsui K, Jiang M, Sakata H, Taira M (2003) Short-term memory and perceptual decision for three-dimensional visual features in the caudal intraparietal sulcus (Area CIP). J Neurosci 23:5486–5495.
Vanduffel W, Fize D, Mandeville JB, Nelissen K, Van Hecke P, Rosen BR, Tootell RB, Orban GA (2001) Visual motion processing investigated using contrast agent-enhanced fMRI in awake behaving monkeys. Neuron 32:565–577.
Vanduffel W, Fize D, Peuskens H, Denys K, Sunaert S, Todd JT, Orban GA (2002) Extracting 3D from motion: differences in human and monkey intraparietal cortex. Science 298:413–415.
Van Essen DC, Drury HA, Dickson J, Harwell J, Hanlon D, Anderson CH (2001) An integrated software suite for surface-based analyses of cerebral cortex. J Am Med Inform Assoc 8:443–459.
Yamamoto J, Ikeda A, Satow T, Matsuhashi M, Baba K, Yamane F, Miyamoto S, Mihara T, Hori T, Taki W, Hashimoto N, Shibasaki H (2004) Human eye fields in the frontal lobe as studied by epicortical recording of movement-related cortical potentials. Brain 127:873–887.